

Renormalization of One-Dimensional Avalanche Models

Jeff Hasty¹ and Kurt Wiesenfeld¹

Received April 8, 1996; final August 15, 1996

We investigate a renormalization group (RG) scheme for avalanche automata introduced recently by Pietronero *et al.* to explain universality in self-organized criticality models. Using a modified approach, we construct exact RG equations for a one-dimensional model whose detailed dynamics is exactly solvable. We then investigate in detail the effect of approximations inherent in a practical implementation of the RG transformation where exact dynamical information is unavailable.

KEY WORDS: Avalanching; self-organized criticality; renormalization group.

1. INTRODUCTION

Since its introduction almost a decade ago,⁽¹⁾ the phenomenon of self-organized criticality (SOC) has been widely studied. A variety of theoretical models have been shown to display SOC behavior: that is, their dynamics naturally evolve to a complicated self-sustaining state in which avalanches of all sizes are observed. Most of this work has focused on identifying (via computer simulations) what properties are necessary to achieve SOC, determining various critical exponents, and exploring whether universality classes exist. Experimentally, increasing attention has been paid to physical systems which exhibit well-defined avalanche events, and there is mounting evidence that some of these show SOC (e.g., refs. 2). Some theoretical effort has been devoted to going beyond simulations, and several distinct approaches have been followed. These include algebraic analysis of Abelian models,⁽³⁾ derivation of a macroscopic singular diffusion equation from an

¹ School of Physics, Georgia Institute of Technology, Atlanta, Georgia 30332; e-mail: jeff@tabkl.gatech.edu, kw2@prism.gatech.edu.

underlying microscopic dynamics,⁽⁴⁾ and a scaling theory for “extremal dynamics” encompassing a variety of avalanching systems.⁽⁵⁾

Recently, Pietronero, Vespignani, and Zapperi (PVZ) conceived a real-space renormalization group theory for SOC⁽⁶⁾ and explicitly implemented the procedure on systems in two dimensions. Their theory explains the existence of universality classes and also allows explicit calculation of certain exponents characterizing the avalanche distribution. While there is still some debate about the proper characterization of SOC universality classes,^(7, 8) PVZ managed to compute the avalanche exponents to impressive accuracy.

The purpose of the present paper is to investigate further the renormalization group approach in the spirit of PVZ. We consider a class of one-dimensional cellular automaton models whose dynamics can be solved exactly, which allows us to (i) construct explicitly exact renormalization group equations and (ii) investigate in detail the approximations inherent in practical implementation of the renormalization group transformation.

An important point is that the validity of the RG approach *does not require* the existence of power law distributions: it is much more powerful. Indeed, the exactly solvable models we consider in this paper display linear avalanche distributions, and though technically a power law, this case is usually viewed as “trivial” in the context of SOC. Nevertheless, the RG approach allows one to calculate (in principle) the complete avalanche distribution regardless of its functional form. An analogous statement is true in applying RG in equilibrium statistical mechanics: most attention is paid to the critical point, but the technique is equally applicable away from it.⁽⁹⁾

2. BACKGROUND

2.1. Renormalization Group Approach

In this section we briefly review the real space renormalization theory of PVZ.⁽⁶⁾ That work gives a framework for understanding universality in SOC models and a procedure for determining theoretically the avalanche distribution. PVZ explicitly constructed a renormalization transformation for a fairly general class of systems in two dimensions, which predicts that different microscopic models correspond to the same coarse-grained model, which is itself scale-invariant and characterized by power law distributions, e.g.,

$$P(s) \sim s^{1-\tau} \quad (2.1)$$

where s is the number of sites affected in a single avalanche, and $P(s)$ is the probability that at least s sites are involved. Such power-law distributions are a defining feature of SOC systems. The PVZ theory predicts a universal value of $\tau = 1.253$, which is in good agreement with values determined from large computer simulations of two distinct models: $\tau = 1.22$ for the original sandpile model of Bak, Tang, and Wiesenfeld (BTW),^(1, 11) and $\tau = 1.28$ for the two-state model introduced by Manna.⁽¹⁰⁾ PVZ therefore explain at once the commonality of the exponents (an indication of universality) and calculate this exponent theoretically, without need for simulations. PVZ explicitly focus on two-dimensional models; however, it is clear how to apply their ideas to systems in any number of dimensions.

The specific steps of the PVZ theory are as follows. First, one defines a space of models so that different models correspond to distinct points in the space. The coordinates in this space are probabilities specifying the relaxation rule. (The analogous situation in traditional critical phenomena is the space of spin-Hamiltonians with coordinates given by the set of coupling constants.) Next, a renormalization operator is defined which relates the dynamics described at one scale to its coarse-grained analog. Application of the renormalization operator induces a discrete map on the space of systems; a fixed point of this map corresponds to a perfectly scale-invariant model. The properties of the fixed point are directly related to the avalanche distribution exponents.

For example, consider systems defined on a two-dimensional square lattice (the case explicitly implemented by PVZ). The space of probabilities p_j^k is defined as the probability that a critical site at scale k will relax by dropping grains to j neighbors ($j = 1, 2, 3, 4$). In the BTW model, critical sites decay by spilling one grain to each of their four nearest neighbors: this is the dynamics at the microscopic level (designated scale $k = 0$) and so $(p_1^0, p_2^0, p_3^0, p_4^0) = (0, 0, 0, 1)$. In the Manna model the relaxation rule is different: critical sites decay by spilling two grains, one grain each to two randomly chosen nearest neighbors, so $(p_1^0, p_2^0, p_3^0, p_4^0) = (0, 1, 0, 0)$.

The next step is to define a renormalization transformation as follows. A cell consisting of four sites is used to calculate the probability that the cell will relax to j neighboring cells in terms of the microscopic p_j^0 . For each cell configuration, one writes p_j^1 in terms of the p_j^0 by summing over all possible paths, then takes a weighted average over all cell configurations. This last step involves a crucial element of the PVZ theory, namely an additional parameter ρ which represents the fraction of critical sites and is itself determined by enforcing "energy balance." Physically, the idea is that any given (coarse-grained) cell must have on average as many grains flowing out as flowing in; otherwise, the system is not in the steady state (i.e., not on the attractor).

In this manner one determines the renormalization equations giving (p_j^1, ρ^1) in terms of (p_j^0, ρ^0) . This readily generalizes to give (p_j^{k+1}, ρ^{k+1}) in terms of (p_j^k, ρ^k) .

PVZ actually show how the (coarse-grained) avalanche distribution can be constructed from any trajectory (p_j^k, ρ^k) ; the special case of a fixed-point trajectory corresponds to an exact power-law distribution. For systems on a two-dimensional square lattice, they find an attractive fixed point at $(\mathbf{p}, \rho) = (0.240, 0.442, 0.261, 0.057, 0.468)$, which corresponds to a power-law avalanche distribution with $\tau = 1.253$. Both the BTW and Manna models are in the basin of attraction of this fixed point, and thus should exhibit this distribution except at the shortest length scales.

We now turn our attention to a simpler cellular automaton which we can solve exactly. We will see that an exact renormalization transformation does not require the imposition of “energy balance”; this is automatically satisfied on the attractor. The coarse-graining procedure of PVZ neglects site-site correlations inherent in the steady state, and the extra balance condition serves to compensate in part for the neglected correlations.

2.2. A Simple 1D Cellular Automaton

The first exactly solvable model we consider is the BTW model in one spatial dimension. By “exactly solvable” we mean that we have complete and explicit knowledge of the attracting dynamics. In particular (i) we can enumerate all stable configurations on the attractor and (ii) for each configuration we can predict precisely the result of dropping one grain on any site. The price we pay is that this model does not exhibit “true SOC”; that is, the avalanche distribution is a linear function and although technically this is a power law (with $\tau = -1$), traditionally the model is considered too simple to qualify as SOC. For our purposes this is not a problem: indeed, it is just this simplicity that allows us to find an exact solution, which in turn lets us understand in detail the renormalization procedure.

On a lattice of length L , we call h_j the number of grains at site j . We choose a random site d and drop a grain on this position

$$h_d \rightarrow h_d + 1 \quad (2.2)$$

If h_d exceeds a threshold value h_c , the site relaxes by passing one grain each to the left and right,

$$\begin{aligned} h_d &\rightarrow h_d - 2 \\ h_{d\pm 1} &\rightarrow h_{d\pm 1} + 1 \end{aligned} \quad (2.3)$$

which can of course destabilize the neighboring sites. The updating is performed in parallel, The relaxation process continues, with updating performed in parallel (i.e., all relaxing sites are updated simultaneously), until all sites are stable, at which time the avalanche is finished. Another grain is then added at a randomly selected site, and so on. The boundary conditions are such that sand leaves the system on both ends. The attracting dynamics is independent of the threshold value; we set $h_c = 1$.

Although not obvious, the above algorithm leads to relatively simple dynamical behavior, which can be completely characterized as follows. There are precisely $L + 1$ recurrent (stable) states.² These are the configurations having at most one site with $h = 0$ and all other sites $h = 1$. We call the $h = 0$ site a trap site; the importance of a trap site is that an avalanche cannot propagate past it.⁽¹²⁾ Starting from any of these $L + 1$ states, a grain can be dropped on any of the L sites, giving a total of $L(L + 1)$ possible avalanches to consider. These fall into three groups: (i) if the initial state is the no-trap state) then the avalanche extends throughout the system (and so has size L) and a single trap is created; (ii) if the initial state has a trap and the drop occurs on the trap, there is no avalanche and the resulting state is the no-trap state; (iii) if the initial state has a trap site, but the drop occurs elsewhere, the avalanche extends from the trap on one side to the system boundary on the other and a new site becomes the trap.

We can summarize the net effect after dropping on site d by a single rule^(12, 13)

$$\begin{aligned}
 h_d &\rightarrow h_d - 1 \\
 h_{r-d+l} &\rightarrow h_{r-d+l} - 1 \\
 h_r &\rightarrow h_r + 1 \\
 h_l &\rightarrow h_l + 1
 \end{aligned}
 \tag{2.4}$$

where r and l denote the trap site to the right and left of the drop site d , respectively, with the convention that $l = 0$ if there is no trap to the left and $r = L + 1$ if there is no trap to the right. The rule (2.4) represents an exact solution to the dynamical system, and its importance lies in its role in allowing us to deduce exact results, including construction of an exact renormalization group transformation in the next section. It is a

² This can also be determined by direct calculation of the determinant of the toppling matrix, following Dhar.⁽¹³⁾

straightforward matter to derive the exact avalanche distribution, with result

$$f(n) = \begin{cases} 1/(L+1) & \text{for } n=0 \\ 2n/L(L+1) & \text{for } 1 \leq n \leq L-1 \\ 1/(L+1) & \text{for } n=L \end{cases} \quad (2.5)$$

where $f(n)$ is the probability that an avalanche affects exactly n sites.

3. A RENORMALIZATION THEORY FOR 1D AUTOMATA

In this section, we construct a renormalization approach similar to PVZ, but with some differences which allow us to exploit our exact knowledge of the dynamics. Applied to the 1d BTW model, we generate exact renormalization equations which recover, for example, the avalanche distribution (2.5). We then show how a natural approximation which ignores site-site correlations affects the results, and how enforcement of a “balance condition” can partially compensate. In Section 4 we extend our results to a family of models.

3.1. Probability Amplitudes

Following PVZ, we begin by defining a space of systems with differing relaxation behavior. A cell consisting of s contiguous sites can be excited in two distinct ways, depending on whether or not it contains the drop site (which initiates the avalanche), and we explicitly distinguish between these.³ We denote by D_j the event where, given that the initial drop site is in the cell, the subsequent avalanche eventually affects j distinct nearest neighbors ($j=0, 1, 2$). We then let $\mathcal{D}_j(s)$ be the probability that a D_j event occurs, and refer to these probabilities as the “drop amplitudes”; of course $\mathcal{D}_0(s) + \mathcal{D}_1(s) + \mathcal{D}_2(s) = 1$. We likewise denote by T_j the event where, given that the initial drop site is not in the cell (and so the cell is initially excited by a “spillage” from a neighboring cell), the cell propagates the avalanche to exactly j distinct nearest neighbor cells. Finally, we let $\mathcal{T}_j(s)$ be the probability that a T_j event occurs, with $\mathcal{T}_0(s) + \mathcal{T}_1(s) + \mathcal{T}_2(s) = 1$. We will refer to these as “transport amplitudes.” As it happens, for our 1D model $\mathcal{T}_2(s)$ is identically zero. Consequently, we have five amplitudes, which are constrained by the two normalization conditions, defining a three-dimensional space of systems. It is in this space that the renormalization group operator acts.

³ Keeping track of this difference is one of the ways that our construction differs from PVZ.

Our next step is to write \mathcal{D}_j and \mathcal{T}_j explicitly in terms of L and s . We can use (2.4) to construct a probability tree for the drop amplitudes, which generates all possible sequences of events after a drop onto a cell. We obtain (see Appendix)

$$\mathcal{D}_0(s) = \frac{1}{L+1} \quad (3.1a)$$

$$\mathcal{D}_1(s) = \frac{s-1}{L+1} \quad (3.1b)$$

$$\mathcal{D}_2(s) = \frac{L+1-s}{L+1} \quad (3.1c)$$

It is easy to see that these are correct at the fundamental scale $s=1$ of the 1D BTW model: $\mathcal{D}_0(1)$ is the probability that the drop site is a trap, and a given site is a trap in precisely one of the $L+1$ stable configurations; $\mathcal{D}_1(1)=0$, since the rule (2.3) never allows spillage to just one neighbor; $\mathcal{D}_2(1)$ is the probability that the drop site is not a trap.

To construct the transport amplitudes, note that once an avalanche begins elsewhere, a cell either stops the avalanche (if it contains a trap site) or the avalanche propagates through the cell (if it contains no trap site). But exactly s of the $L+1$ stable configurations have a trap in a given cell of size s , so

$$\mathcal{T}_0(s) = \frac{s}{L+1} \quad (3.2a)$$

$$\mathcal{T}_1(s) = \frac{L+1-s}{L+1} \quad (3.2b)$$

From these amplitudes we can calculate the avalanche distribution. Let $P(a < s)$ equal the probability that an avalanche affects fewer than s sites. There are two ways that an avalanche can fail to propagate beyond a cell of size s : (i) the drop cell relaxes with a D_0 event or (ii) the drop cell relaxes via a D_1 event, but the cell happens to be adjacent to the system boundary and the transported grain simply spills out of the system. These alternatives are mutually exclusive, so

$$P(a < s) = \mathcal{D}_0(s) + \left(\frac{s}{L}\right) \mathcal{D}_1(s) \quad (3.3)$$

Using (3.1), we get

$$P(a < s) = \frac{1}{L+1} + \frac{s}{L} \left(\frac{s-1}{L+1} \right) \tag{3.4}$$

which agrees with (2.5) for all $s \leq L$, as it must.

3.2. Exact Renormalization Equations

We now carry out a coarse-graining procedure. We look at two adjacent cells of size s and seek to write \mathcal{D}'_j and \mathcal{T}'_j for this composite cell in terms of the unprimed probabilities at scale s . For example, in calculating \mathcal{D}'_0 , we consider the combinations of \mathcal{D}_i and \mathcal{T}_j which lead to no spillage out of the two-cell block (see Fig. 1). We obtain

$$\mathcal{D}'_0 = \mathcal{D}_0 + \frac{1}{2} \text{PROB}(D_1 \cap T_0) \tag{3.5}$$

where the first term represents the path where the dropped grain happens to land on the trap, and the second one that where the drop caused an "internal" spill, which, however, fails to propagate through the composite cell; the latter involves the joint probability of two consecutive events (denoted by the symbol \cap). This joint probability can be reexpressed as the product

$$\text{PROB}(D_1 \cap T_0) = \mathcal{D}_1 \cdot \text{PROB}(T_0|D_1) \tag{3.6}$$

where $\text{PROB}(T_0|D_1)$ denotes the conditional probability that a T_0 event occurs, *given* that a D_1 event precedes it. For this model, this term is zero

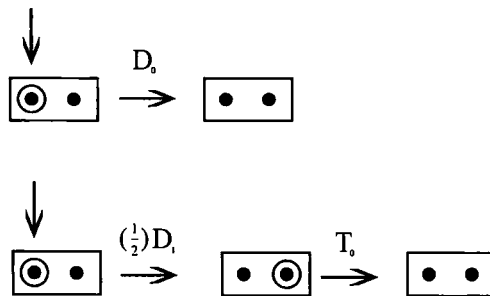


Fig. 1. Example of the renormalization scheme. The filled circle represents a critical (but stable) site; the additional ring denotes a supercritical site which must then relax. Shown are the two dynamical paths for which no grains spill out of the composite cell, corresponding to the two terms for the composite amplitude \mathcal{D}'_0 .

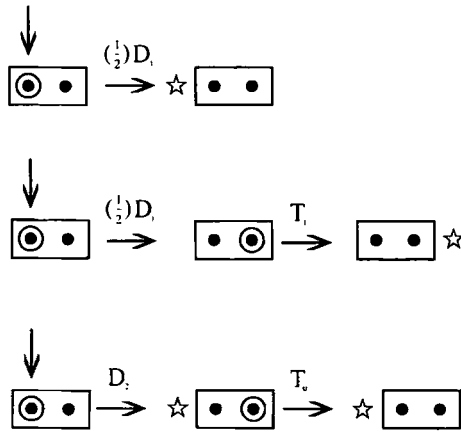


Fig. 2. The three dynamical paths generating \mathcal{S}'_1 .

since both events require a trap, and there are no configurations on the attractor with two traps. Therefore,

$$\mathcal{D}'_0 = \mathcal{D}_0 = \frac{1}{L+1} \tag{3.7}$$

In a similar way we calculate \mathcal{D}'_1 (see Fig. 2),

$$\begin{aligned} \mathcal{D}'_1 &= \text{PROB}(D_2 \cap T_0) + \frac{1}{2}\mathcal{D}_1 + \frac{1}{2}\text{PROB}(D_1 \cap T_1) \\ &= \mathcal{D}_2 \cdot \text{PROB}(T_0 | D_2) + \frac{1}{2}\mathcal{D}_1 + \frac{1}{2}\mathcal{D}_1 \cdot \text{PROB}(T_1 | D_1) \\ &= \mathcal{D}_2(s) \cdot \mathcal{T}_0(s, L-s) + \frac{1}{2}\mathcal{D}_1(s) + \frac{1}{2}\mathcal{D}_1(s) \cdot 1 \end{aligned} \tag{3.8}$$

where the notation $\mathcal{T}_j(s, L-s)$ denotes the corresponding expression (3.2) with the substitution $L \rightarrow L-s$. [That $\text{PROB}(T_0 | D_2) = \mathcal{T}_j(s, L-s)$ follows, since a D_2 event requires no trap in the cell, i.e., that the trap—if any—must lie among the remaining $L-s$ sites.] Similarly, we have

$$\mathcal{D}'_2 = \text{PROB}(D_2 \cap T_1) = \mathcal{D}_2 \cdot \mathcal{T}_1(s, L-s) \tag{3.9}$$

In a like manner we can renormalize the \mathcal{T}_j . Since an avalanche either stops at the first cell in the block of two or propagates and stops at the second, we have

$$\begin{aligned} \mathcal{T}'_0 &= \mathcal{T}_0 + \text{PROB}(T_1 \cap T_0) \\ &= \mathcal{T}_0(s) + \mathcal{T}_1(s) \cdot \mathcal{T}_0(s, L-s) \end{aligned} \tag{3.10}$$

Lastly,

$$\begin{aligned}\mathcal{F}'_1 &= \text{PROB}(T_1 \cap T_1) \\ &= \mathcal{F}_1(s) \cdot \mathcal{F}_1(s, L-s)\end{aligned}\quad (3.11)$$

Equations (3.7)–(3.11) give the five coarse-grained amplitudes \mathcal{D}'_j and \mathcal{F}'_j . If the renormalization is exact, then the coarse-grained amplitudes for composite cells should be identical to the original amplitudes evaluated at cell size $2s$, i.e., $\mathcal{O}'_j = \mathcal{O}_j(2s)$ for any amplitude \mathcal{O}_j . This is readily verified using expressions (3.1) and (3.2).

We make one more observation. On the attractor, the number of grains entering any cell must on average equal the amount leaving it. In terms of two of the amplitudes this “balance condition” can be written (see Appendix)

$$\mathcal{F}_0 = 1 - \mathcal{D}_2 \quad (3.12)$$

Notice that this condition is automatically satisfied; cf. Eqs. (3.1) and (3.2).

3.3. Approximate Renormalization

The exact results (3.7)–(3.12) make intimate use of our complete knowledge of the dynamics: we enumerated all recurrent configurations and all possible avalanches connecting them. Said differently, we use *global information* about the dynamics on the attractor, which is crucial for getting exact results. In contrast, PVZ use only local dynamics, which inevitably throws out information. Despite its approximate nature, however, a local construction is preferred as a practical matter since exact global knowledge is not typically available. Of course, not any local construction will do: it must be quantitatively accurate.

Armed with our exact solution, we can investigate in some detail what happens when global knowledge of the attractor is ignored and how the resulting approximations can be improved. In particular, without information about correlations we cannot evaluate exactly the joint probabilities $\text{PROB}(O_i \cap O_j)$ in (3.7)–(3.11). The most straightforward approach is to *ignore* correlations altogether and write $\text{PROB}(O_i \cap O_j) \approx \mathcal{O}_i \cdot \mathcal{O}_j$, in which case we obtain

$$\mathcal{D}'_0 = \mathcal{D}_0 + \frac{1}{2}\mathcal{D}_1 \cdot \mathcal{F}_0 \quad (3.13a)$$

$$\mathcal{D}'_1 = \mathcal{D}_2 \cdot \mathcal{F}_0 + \frac{1}{2}\mathcal{D}_1 + \frac{1}{2}\mathcal{D}_1 \cdot \mathcal{F}_1 \quad (3.13b)$$

$$\mathcal{D}'_2 = \mathcal{D}_2 \cdot \mathcal{F}_1 \tag{3.13c}$$

$$\mathcal{F}'_0 = \mathcal{F}_0 + \mathcal{F}_1 \cdot \mathcal{F}_0 \tag{3.13d}$$

$$\mathcal{F}'_1 = \mathcal{F}_1 \cdot \mathcal{F}_1 \tag{3.13e}$$

When iterated, the above equations diverge from the exact solution. This divergence can be corrected to some degree by imposing the balance condition (3.12) at each iteration step. For example, at each iteration we determine the \mathcal{D}_j amplitudes using (3.13), then impose the balance constraint (3.12) to determine \mathcal{F}'_0 , and finally use normalization (i.e., $\mathcal{F}'_0 + \mathcal{F}'_1 = 1$) to determine \mathcal{F}'_1 .

Figure 3 compares the renormalization of the drop and transport amplitudes for three different schemes: using the exact equations, using the approximate equations (3.13) directly without concern for balance, and finally using the approximate equations for the drop amplitudes with balance determining the transport operators as just described. This last

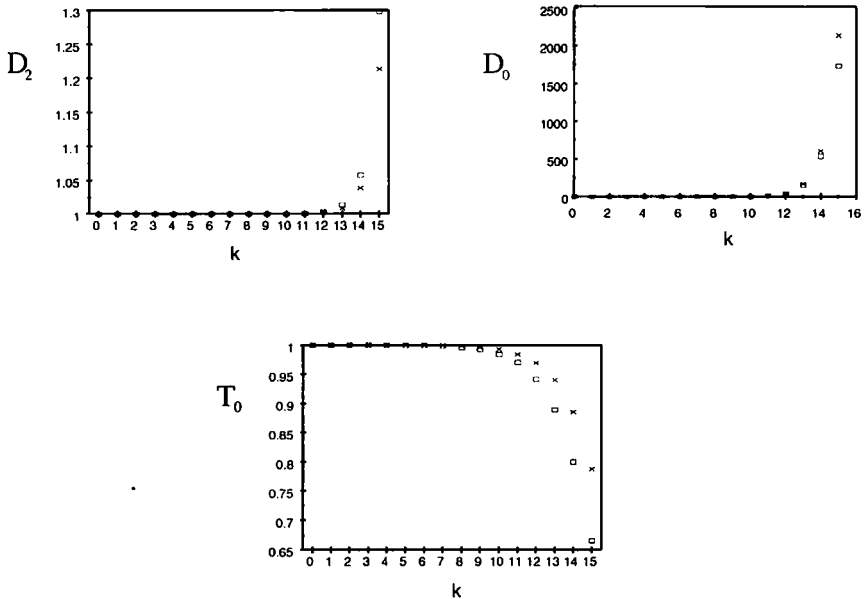


Fig. 3. Comparison of the probability amplitudes generated in the two approximate RG maps. Plotted are $\mathcal{C}_j/\mathcal{C}_j^{(exact)}$, with \mathcal{C}_j determined using the approximate RG equations (\square), and the balance-augmented RG equations (\times) ($s=2^k$).

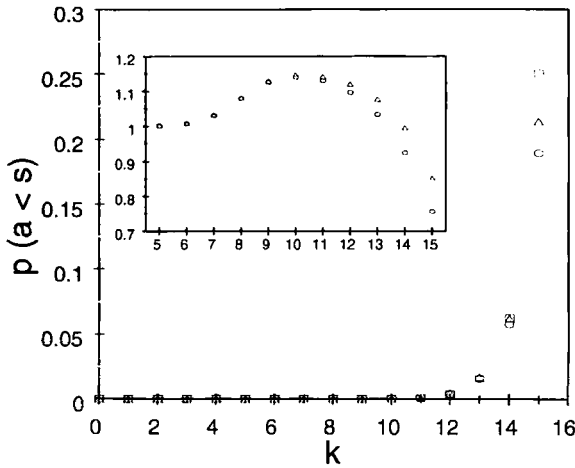


Fig. 4. Comparison of $P(a < s)$, obtained using exact RG equations (\square), approximate RG equations (\circ), and the balance-augmented RG equations (\triangle).

approach amounts to using (3.12) to eliminate the transport operators from (3.13). Explicitly, this yields the following map:

$$\mathcal{D}_0^{(k+1)} = \mathcal{D}_0^{(k)} + \frac{1}{2}\mathcal{D}_1^{(k)}(1 - \mathcal{D}_2^{(k)}) \tag{3.14a}$$

$$\mathcal{D}_1^{(k+1)} = \mathcal{D}_2^{(k)}(1 - \mathcal{D}_2^{(k)}) + \frac{1}{2}\mathcal{D}_1^{(k)} + \frac{1}{2}\mathcal{D}_1^{(k)}\mathcal{D}_2^{(k)} \tag{3.14b}$$

$$\mathcal{D}_2^{(k+1)} = \mathcal{D}_2^{(k)}\mathcal{D}_2^{(k)} \tag{3.14c}$$

where we impose normalization after each iteration.

Figure 4 shows the corresponding results for the predicted avalanche distribution. Using the probability amplitudes from Fig. 3, we evaluate (3.3) to get $P(s < a)$.

4. A FAMILY OF MIXED MODELS

The 1D BTW model corresponds to a particular point in the three-dimensional system space, namely

$$(\mathcal{D}_0, \mathcal{D}_2, \mathcal{F}_0) = \left(\frac{1}{L+1}, \frac{L}{L+1}, \frac{1}{L+1} \right)$$

So far we have focused on how the renormalization equations act on this initial condition; we have investigated only a single trajectory in the space.

We now generalize to a family of 1D models. Each member of the family corresponds to a different initial condition for the renormalization transformation. These models still behave simply enough that we can solve exactly the dynamics on the attractor. We present exact renormalization equations which can be used to derive the avalanche distribution, and then compare this with approximate renormalization equations with and without enforcing a balance condition.

4.1. The Model

The generalized model differs only in the relaxation rule, which depends on a single parameter q . On a lattice of length L , we choose a random site d and drop a grain on it by letting $h_d \rightarrow h_d + 1$. When the height becomes greater than $h_c = 1$, the site relaxes as follows. With probability q , the rule is (2.3)

$$\begin{aligned} h_d &\rightarrow h_d - 2 \\ h_{d\pm 1} &\rightarrow h_{d\pm 1} + 1 \end{aligned} \quad (4.1)$$

With probability $(1 - q)/2$, it relaxes according to

$$\begin{aligned} h_d &\rightarrow h_d - 1 \\ h_{d+1} &\rightarrow h_{d+1} + 1 \end{aligned} \quad (4.2)$$

and with probability $(1 - q)/2$, it relaxes according to

$$\begin{aligned} h_d &\rightarrow h_d - 1 \\ h_{d-1} &\rightarrow h_{d-1} + 1 \end{aligned} \quad (4.3)$$

Once the avalanche has started, the same relaxation rule is applied for the remainder of the avalanche, until all sites are stable. We then repeat the process. The 1D BTW model corresponds to the special case $q = 1$. In Fig. 5, we plot the avalanche distribution obtained from simulations of this "mixed rule" for $q = 0.95$.

In fact, for any value of $q > 0$ the recurrent configurations are just as before: a static pile either contains one or no traps. We can see this since the net effect of (4.2), (4.3) is simply to fill in a trap or propagate off the system boundary. This fact is useful in the derivation of the results below. Unlike the $q = 1$ case, however, the trapless configuration recurs more frequently than any of the one-trap configurations.

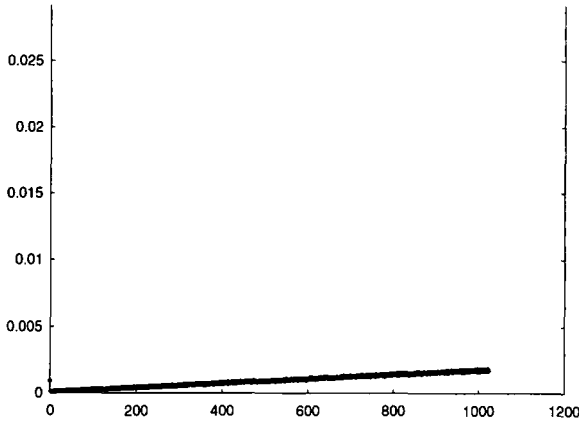


Fig. 5. Avalanche distribution $P(a)$ for the generalized model with $q = 0.95$.

We now express the operators \mathcal{D}_j and \mathcal{T}_j explicitly as functions of q , s , and L . Following the same procedure as before—generating all possible paths—we obtain the analogues of (3.1) (see Appendix):

$$\mathcal{D}_0 = p_t \left(\frac{1}{L} \right) + (1 - q) p_t \left(\frac{s - 1}{2L} \right) \tag{4.4a}$$

$$\mathcal{D}_1 = qp_t \left(\frac{s - 1}{L} \right) + (1 - q) \left(1 - \frac{(s + 1) p_t}{2L} \right) \tag{4.4b}$$

$$\mathcal{D}_2 = q \left(1 - \frac{sp_t}{L} \right) \tag{4.4c}$$

where $p_t \equiv 2qL / (L + 2q + Lq)$ is the probability that a given stable configuration contains a trap. Of course, these equations reduce to (3.1) in the $q = 1$ limit.

To find the transport amplitudes, note that an avalanche propagates through a cell if either (i) the configuration contains no trap or (ii) the configuration contains a trap, but the trap is not in the given cell. Conversely, an avalanche is stopped if the trap exists and is in the cell. Therefore

$$\mathcal{T}_0(s) = p_t \frac{s}{L} \tag{4.5a}$$

$$\mathcal{T}_1(s) = (1 - p_t) + p_t \left(\frac{L - s}{L} \right) \tag{4.5b}$$

Expressions (4.4) and (4.5) can be checked by direct comparison with simulations: the agreement is excellent.

Our next step is to relate the drop and transport amplitudes to the avalanche distribution. For the generalized model this expression involves three terms rather than only two for the $q = 1$ case [cf. (3.3)],

$$P(a \leq s) = \mathcal{D}_0(s)(s) + \left(\frac{s}{L}\right) \mathcal{D}_1(s) + \left(1 - \frac{2s}{L}\right) \text{PROB}(D_1 \cap T_0) \quad (4.6)$$

In the earlier model, an avalanche failed to propagate beyond the composite cell if either (i) the drop site was a trap or (ii) the drop cell was a boundary cell and relaxed via a D_1 event. But the generalized model admits another path, corresponding to the last term in the above expression, whereby the drop cell is a nonboundary cell (probability $1 - 2s/L$ for $s < L/2$) and the relaxation sequence is D_1 followed by T_0 . The probability of having this last term is zero if $q = 1$.

To evaluate the joint probability $\text{PROB}(D_1 \cap T_0)$, we can consider the two mutually exclusive cases

$$\text{PROB}(D_1 \cap T_0) = \text{PROB}(D_1 \cap T_0 \cap 1) + \text{PROB}(D_1 \cap T_0 \cap 2) \quad (4.7)$$

where “1” and “2” denote that the (randomly chosen) relaxation rule involves one or two grains, respectively. Of course, this second case is precisely the situation in the earlier model: both D_1 and T_0 events require traps and so that term is zero. On the other hand,

$$\begin{aligned} \text{PROB}(D_1 \cap T_0 \cap 1) &= \text{PROB}(D_1 \cap 1 \cap T_0) \\ &\approx \text{PROB}(D_1 \cap 1) \cdot \mathcal{T}_0 \\ &= (1 - q) \left(1 - p_i \frac{s}{2L}\right) \mathcal{T}_0 \end{aligned} \quad (4.8)$$

where we have used the fact that $\text{PROB}(D_1 \cap 1)$ corresponds to the second term of Eq. (4.4b).

The above considerations finesse one technical point associated with coarse graining: the path $D_1 \cap T_0$ actually contributes to avalanche sizes from $s = 1$ all the way up to $2s - 1$, whereas we want only the fraction f which accounts for avalanches of size s or less. We can account for this by taking

$$f = \frac{\sum_{k=1}^s k}{\sum_{k=1}^{2s-1} k} = \frac{s^2}{3s^2 - 3s + 1} \quad (4.9)$$

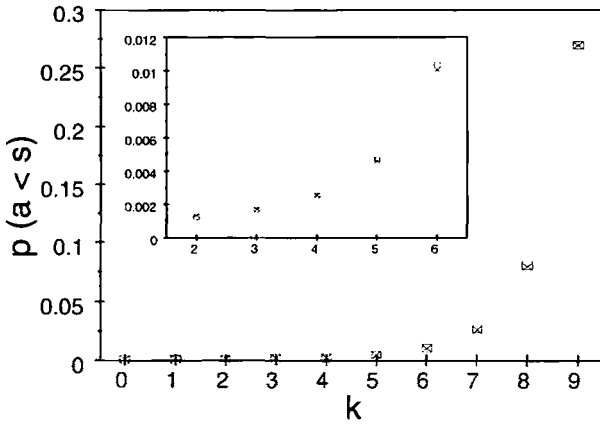


Fig. 6. Comparison of $P(a \leq s)$ for the generalized model with $q=0.95$. Direct simulation (\square) and theoretical results (\times).

which assumes a linear avalanche distribution, consistent with simulations. Putting this all together yields

$$p(a \leq s) = \mathcal{D}_0(s) + \left(\frac{s}{L}\right) \mathcal{D}_1(s) + \frac{s^2}{3s^2 - 3s + 1} (1 - q) \left(1 - p_c \frac{s + 1}{2L}\right) \mathcal{T}_0(s) \tag{4.10}$$

Figure 6 compares (4.10) with the avalanche distribution obtained from direct simulations for $q = 0.95$. The agreement is excellent.

4.2. Renormalization Equations Applied to the Mixed Model

The RG approach gives us an alternative way to calculate the avalanche distribution. In fact, though presented in the context of the pure case $q = 1$, the RG equations (3.13) are equally valid for the mixed model. Recall that these were derived ignoring site-site correlations; as before we can try to compensate for this by imposing a balance condition appropriate for the generalized model:

$$\mathcal{T}_0 = 1 - \left(\frac{1}{q}\right) \mathcal{D}_2 \tag{4.11}$$

which is automatically satisfied on the attractor in the exact treatment (see Appendix A2).

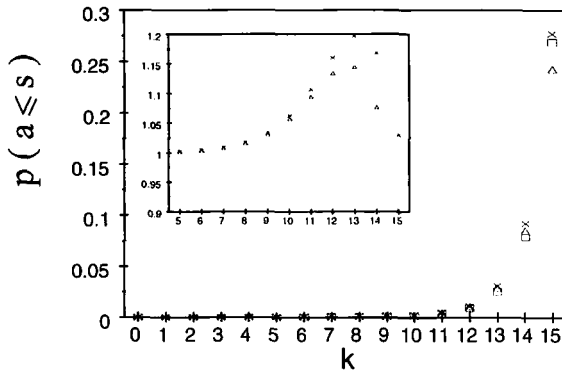


Fig. 7. Comparison of $P(a < s)$ with $q=0.95$, obtained using exact RG equations (\square), approximate RG equations (\times), and the balance-augmented RG equations (\triangle).

Figure 7 shows the avalanche distribution for the model with $q=0.95$. Shown are the results of direct simulations, together with the derived results (4.10) and those determined via the RG map (3.13) both with and without imposing the balance condition (4.11). (The balance-corrected RG map is generated precisely as in Section 3.) The shown behavior is typical of that found for other values of q .

5. SUMMARY AND CONCLUSIONS

In this paper we implemented a real-space renormalization group scheme for a class of cellular automaton avalanche models in one spatial dimension. These relatively simple models are well suited for exploring the RG framework, since they are exactly solvable in the dynamical systems sense. This allowed us to construct (in one case) an exact RG transformation and to explore the effect of practical approximations in some detail.

Although primarily motivated by the work of Pietronero, Vespignani, and Zapperi for two-dimensional systems, our scheme involved modifications which allowed us to exploit our complete knowledge of the dynamics on the attractor. An important aspect of the PVZ theory is that the RG approach allowed us to reconstruct the (size) avalanche distribution independent of whether or not the distribution happens to be a power law. Indeed, for our purposes the functional form is a minor detail, though of course it is a significant issue for the larger study of self-organized criticality.

One of our main results was to clarify the role of the “balance condition” in the renormalization scheme, which in the PVZ theory is a central element, yet enters in a somewhat *ad hoc* way. We saw that in an exact treatment, balance is automatically satisfied; it does not need to be

imposed as an auxiliary condition. Its role is to compensate, in a rough way, for site-site correlations automatically ignored in deriving the RG transformation. Said differently, imposing balance is a way to differentially weight various microscopic configurations—in the language of dynamical systems theory, it amounts to preferentially weighting configurations lying on the *phase-space attractor*, which is the only part that determines the steady-state behavior. This viewpoint is different from (and perhaps complementary to) the one forwarded by PVZ, who interpreted the balance condition as providing a nonlinear feedback mechanism directly responsible for the self-organization in these systems.

Although our view is that the balance condition is not fundamental, because it is an automatic consequence of the attracting dynamics, we also emphasize that it is absolutely crucial in a practical sense. This is because we almost never have complete global dynamical information necessary to construct the attractor. Instead, a balance condition is a straightforward way of including at least one piece of global information about the attractor. In this way the RG approach becomes a practical tool for studying the statistics of these avalanching systems.

We note that still more can be done with these 1D models. In particular, the description embodied by Eq. (2.4) is valid not only on the attractor, but during the transient evolution as well. It would be very interesting if the RG picture could be broadened to include the transient approach to the final attractor, a process at the heart of the self-organizing aspect of self-organized criticality.

Also of interest is the fundamental issue of whether the RG picture can be reconciled with the nonuniversal behavior observed in certain avalanche models, such as the mass-conserving Abelian models on decorated lattices⁽¹⁴⁾ and nonconserving models.⁽⁸⁾ Perhaps not, but in principle it is possible. Although discrete maps have isolated fixed points, a map can have an entire line of fixed points, which would correspond to a continuous range of critical exponents. The RG map studied in this paper does not, but a generalization to a higher dimensional phase space might have this property. [The additional coordinate(s) might distinguish, e.g., different decorations or the degree of nonconservation.] If so, identifying the special property or symmetry responsible for the degenerate fixed-point structure would be a key step toward a comprehensive theory of these avalanching systems.

APPENDIX

A1. Probability Amplitudes $\mathcal{D}_j(s)$

Define S as the set of sites in a cell of size s . Without loss of generality, we set $l=0$ and $r=t$, so that the drop site d is always to the left of the

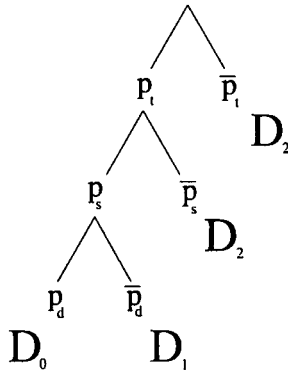


Fig. 8. Probability tree for the 1D BTW model.

trap t . If we drop on a site other than the trap, (2.4) gives the new trap site $t' = t - d$.

To keep track of all possible paths generated from dropping a grain onto S ($d \in S$), we construct the tree shown in Fig. 8. At each level of the tree, beginning with the node at the top, one may choose any branch, each representing a distinct event in the relaxation history of the composite cell S . Every complete path terminates at one of the roots: the labels \mathcal{D}_0 , \mathcal{D}_1 , and \mathcal{D}_2 denote that a path ending at a particular root contributes to that particular drop amplitude for the composite cell. From Fig. 8 we see that there are four distinct paths, two contributing to \mathcal{D}_2 and one each to \mathcal{D}_0 and \mathcal{D}_1 . We have

$$\begin{aligned}
 \mathcal{D}_0 &= p_t \cdot p_s \cdot p_d \\
 \mathcal{D}_1 &= p_t \cdot p_s \cdot \bar{p}_d \\
 \mathcal{D}_2 &= p_t \cdot \bar{p}_s + \bar{p}_t
 \end{aligned}
 \tag{A1}$$

where p_t is the probability of a trap being present anywhere in the system just before the drop, p_s is the probability that, given that a trap exists, the trap is in S , and p_d is the probability that the dropped grain falls on the trap site, given that a trap exists and $t \in S$. The overbar denotes negation, i.e., \bar{p}_t denotes the probability that a trap does *not* exist prior to a drop.

On the attractor, there are L stable configurations with one trap and one configuration with no traps. All $L + 1$ configurations have equal weight, so that

$$p_t = \frac{\text{number of trap configurations}}{\text{number of configurations}} = \frac{L}{L + 1}
 \tag{A2}$$

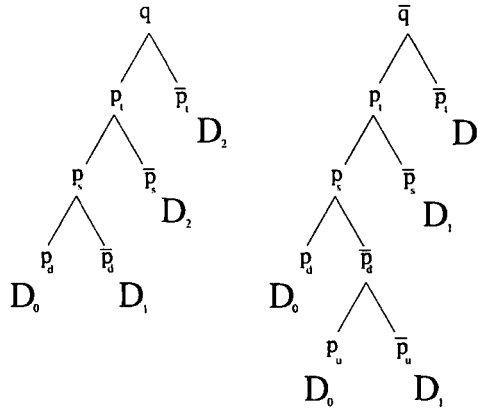


Fig. 9. Probability tree for the generalized model.

The trap can be in any cell with equal likelihood, so

$$p_s = \frac{\text{size of cell}}{\text{length of lattice}} = \frac{s}{L} \tag{A3}$$

The probability of dropping on it is then simply

$$p_d = 1/s \tag{A4}$$

Combining Eqs. (A1)–(A4) yields the quoted result, Eq. (3.1).

For the mixed model the relevant tree (Fig. 9) has an extra level; the top-level nodes q and \bar{q} represent the likelihood that the relaxation rule is (4.1) or (4.2), (4.3), respectively. Define p_u as the conditional probability that, given \bar{q} , p_t , p_s , and \bar{p}_d , the transported grain propagates in the direction of the trap site; by symmetry $p_u = \bar{p}_u = 1/2$.

Since d is random, $p_s = s/L$ and $P_d = 1/s$ as before; however, the trapless site occurs more often, so that p_t is different. Leaving p_t undetermined for now (see below), we calculate the drop amplitudes by summing over the relevant paths in Fig. 9, with result

$$\begin{aligned} \mathcal{D}_0 &= p_t \left(\frac{1}{L} \right) + (1 - q) p_t \left(\frac{s - 1}{2L} \right) \\ \mathcal{D}_1 &= qp_t \left(\frac{s - 1}{L} \right) + (1 - q) \left(1 - \frac{(s + 1) p_t}{2L} \right) \\ \mathcal{D}_2 &= q \left(1 - \frac{sp_t}{L} \right) \end{aligned} \tag{A5}$$

A2. The Balance Condition

First consider the pure model ($q = 1$). A cell gains a grain, with probability P_g , if either (i) a trap exists, the trap is in the cell, and we drop on the trap; or (ii) a trap exists and the trap is in the cell, the drop is not on the cell, and the new trap is *not* in the cell:

$$P_g = p_t \cdot p_s \cdot p_d + p_t \cdot p_s \cdot \overline{p_d} \cdot \overline{p_t} \tag{A6}$$

where $p_{t'}$ is the probability that the new trap t' is in the cell. Since t and t' are uncorrelated, $p_t = p_{t'}$ and so from (A2)–(A4) we find

$$P_g = \frac{s}{L} \frac{L - s + 1}{L + 1} \tag{A7}$$

Next, a cell loses a grain with probability P_l if either (i) a trap exists, the trap is not in the cell, and the new trap t' is in the cell; or (ii) a trap does not exist and t' is in the cell:

$$P_l = p_t \cdot \overline{p_s} \cdot p_{t'} + \overline{p_t} \cdot p_{t'} = \frac{s}{L} \frac{L - s + 1}{L + 1} \tag{A8}$$

Note that $P_g = P_l$, so that balance is automatically satisfied on the attractor.

To express the balance equation in terms of the \mathcal{D}_j and \mathcal{T}_j , note first that \mathcal{T}_0 is just the probability that $t \in S$. Define $\hat{\mathcal{T}}_0$ as the probability that $t' \in S$; then $\mathcal{T}_0 = \hat{\mathcal{T}}_0$, since t and t' are uncorrelated. Now, the cell gains a grain only if both $t \in S$ and $t' \ni S$, so that

$$P_g = \mathcal{T}_0(1 - \hat{\mathcal{T}}_0) = \mathcal{T}_0(1 - \mathcal{T}_0) \tag{A9}$$

The cell loses a grain it suffers a D_2 event and $t' \in S$:

$$P_l = \mathcal{D}_2 \hat{\mathcal{T}}_0 = \mathcal{D}_2 \mathcal{T}_0 \tag{A10}$$

Setting $P_g = P_l$ yields

$$\mathcal{T}_0 = 1 - \mathcal{D}_2 \tag{A11}$$

in agreement with (3.1) and (3.2).

For the generalized model, P_g is the weighted sum of two disjoint cases: (i) relaxation occurs according to (4.1) with weight q , in which case (6) gives the probability, or (ii) the relaxation occurs according to

(4.2)–(4.3) with weight \bar{q} , in which case the ceil gains if a trap exists and $t \in S$, and the propagation is toward S. Thus

$$\begin{aligned} P_g &= q(p_t \cdot p_s \cdot p_d + p_t \cdot p_s \cdot \bar{p}_d \cdot \bar{p}_r) + (1-q)(p_t \cdot p_s \cdot p_r) \\ &= qp_t \frac{1}{L} \frac{(s-1)(L-s)}{L^2} + (1-q) p_t \frac{s}{L} \frac{1}{2} \end{aligned} \quad (\text{A12})$$

Meanwhile, since rule (4.2) never leads to a loss of sand, P_l is just the product of the weight q and (A11),

$$\begin{aligned} P_l &= q(p_t \cdot \bar{p}_s \cdot p_r + \bar{p}_t \cdot p_r) \\ &= qp_t \frac{L-s}{L} \frac{s}{L} + (1-p_t) \frac{s}{L} \end{aligned} \quad (\text{A13})$$

Setting $P_g = P_l$ yields

$$p_t = \frac{2Lq}{L + 2q + qL} \quad (\text{A14})$$

and comparison with the expression for \mathcal{D}_2 in (A5) suggests the apparent analogue of (3.12):

$$\mathcal{F}_0 = 1 - \frac{1}{q} \mathcal{D}_2 \quad (\text{A15})$$

Note that (A14) and (A5) imply $\mathcal{D}_2/q \rightarrow 1$ as $q \rightarrow 0$.

ACKNOWLEDGMENTS

We thank Adam Landsberg for stimulating discussions and a critical reading of the manuscript. This work was supported by the Office of Naval Research under grant no. N00014-91-J-1257.

REFERENCES

1. P. Bak, C. Tang, and K. Wiesenfeld, *Phys. Rev. Lett.* **59**:381 (1987); *Phys. Rev. A* **38**:364 (1988).
2. H. J. S. Feder and J. Feder, *Phys. Rev. Lett.* **66**:2669 (1991); S. Field, J. Witt, F. Nori, and X. Ling, *Phys. Rev. Lett.* **74**:1209 (1995); V. Frette, K. Christensen, A. Malthe-Sorensen, J. Feder, T. Jossang, and P. Meakin, *Nature* **379**:49 (1996).
3. D. Dhar, *Phys. Rev. Lett.* **64**:1613 (1990); S. N. Majumdar and D. Dhar, *Physica A* **185**:129 (1992); P. Bak and M. Creutz, in *Fractals and Disordered Systems*, Vol. II, A. Bunde and S. Havlin, eds. (Springer, Berlin, 1994).

4. J. M. Carlson, J. T. Chayes, E. R. Grannan, and G. H. Swindle, *Phys. Rev. Lett.* **65**:2547 (1990); J. M. Carlson, E. R. Grannan, C. Singh, and G. H. Swindle, *Phys. Rev. E* **48**:688 (1993).
5. M. Paczuski, S. Maslov, and P. Bak, Avalanche dynamics in evolution, growth, and depinning models, *Phys. Rev. E* **53**:414 (1996).
6. L. Pietronero, A. Vespignani, and S. Zapperi, *Phys. Rev. Lett.* **72**:1690 (1994); A. Vespignani, S. Zapperi, and Pietronero, *Phys. Rev. E* **51**:1711 (1995).
7. A. Ben-Hur and O. Biham, *Phys. Rev. E* **53**:R1317 (1996);
8. Z. Olami, H. J. S. Feder, and K. Christensen, *Phys. Rev. Lett.* **68**:1244 (1992).
9. Maris and L. P. Kadanoff, *Am. J. Phys.* **46**:652 (1978).
10. S. S. Manna, *J. Phys. A* **24**:L363 (1991).
11. S. S. Manna, *J. Stat. Phys.* **59**:509 (1990); *Physica A* **179**:249 (1991).
12. A. P. Chhabra, M. J. Feigenbaum, L. P. Kadanoff, A. J. Kolan, and I. Procaccia, *Phys. Rev. E* **47**:3099 (1993).
13. J. M. Carlson, J. T. Chayes, E. R. Grannan, and G. H. Swindle, *Phys. Rev. A* **42**:2467 (1990).
14. A. A. Ali and D. Dhar, *Phys. Rev. E* **51**:R2795 (1995).